SAMD9 senses cytosolic double-stranded nucleic acids in epithelial and mesenchymal cells to induce antiviral immunity

Gaopeng Hou, Siyuan Ding *et al.*

Supplementary Figures and Legends

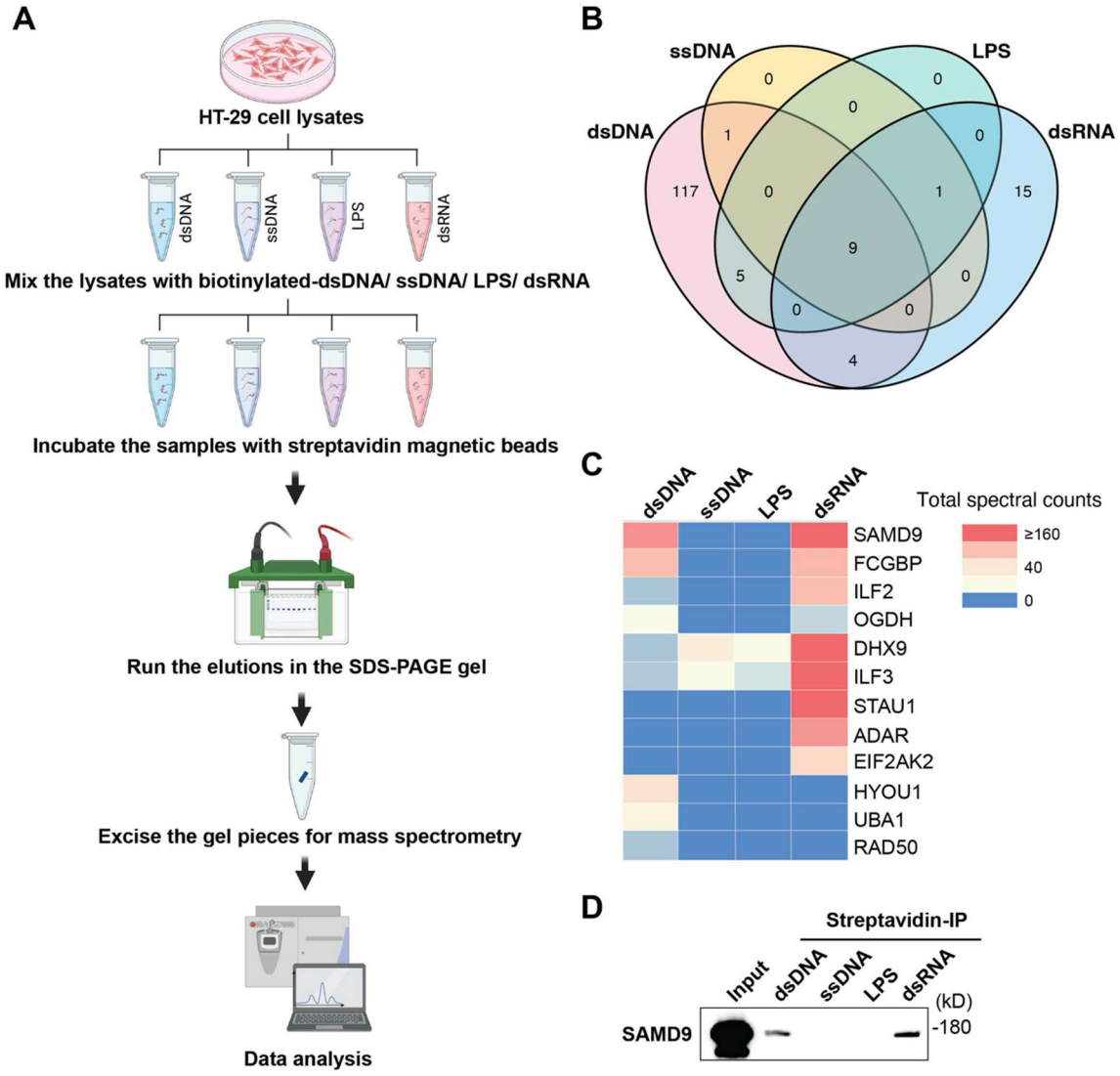

Supplementary Figure 1. Proteomics analysis of host proteins that co-precipitate dsDNA and dsRNA

(A) A workflow diagram of streptavidin-based immunoprecipitation to unbiasedly screen for host proteins that bind to dsDNA- and dsRNA molecules. The schematic illustration was created in BioRender. Hou, G. (2025) https://BioRender.com/p7x5yx3.

(B) A Venn diagram of total number of proteins from biotinylated dsDNA/ ssDNA/ LPS/ dsRNA immunoprecipitated groups. Host proteins with total spectral counts greater than 10 are shown.

(C) Heatmap of representative host proteins enriched in different groups. Note that DHX9, ADAR, and EIF2AK2 (also known as PKR) are well-defined dsRNA binding proteins.

(D) Immunoblotting analysis of streptavidin immunoprecipitates of cell lysates from WT HT-29 incubated with biotinylated dsDNA/ ssDNA/ LPS/ dsRNA. Experiment A was performed once, and experiment D was repeated at least three times.

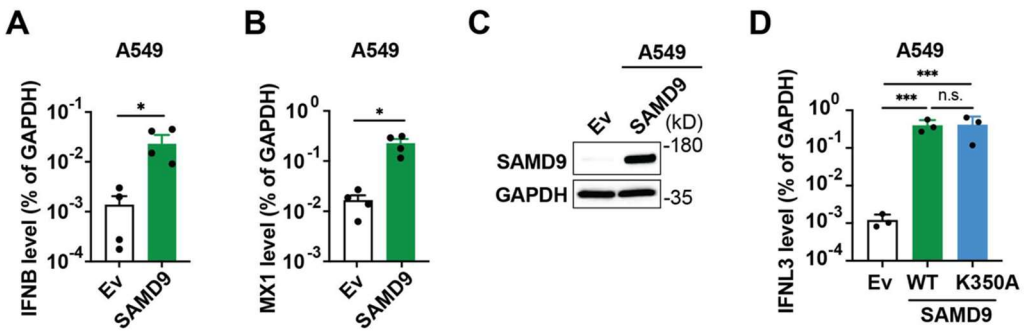

Supplementary Figure 2. SAMD9 induces IFN and ISG expression in A549 cells
(A-B) A549 cells transfected with Ev or SAMD9-Myc-DDK for 24 hr and the mRNA levels of IFNB (A) and MX1 (B) measured by qRT-PCR.
(C) Similar to A except the SAMD9 protein level measured by western blot.
(D) A549 cells transfected with Ev, SAMD9-Myc-DDK (WT), or SAMD9-K350A-Myc-DDK (K350A) plasmid for 24 hr and the mRNA levels of IFNL3 measured by qRT-PCR. For all figures, experiments were repeated at least three times. Individual points in (A, B, and D) represent independent experiments. Data are represented as mean ± SEM. Statistical significance calculated by unpaired two-tailed Student's *t* test (A and B), or one-way ANOVA with Tukey's post-test (D): n.s., not significant, **P* < 0.05, ****P* < 0.001.

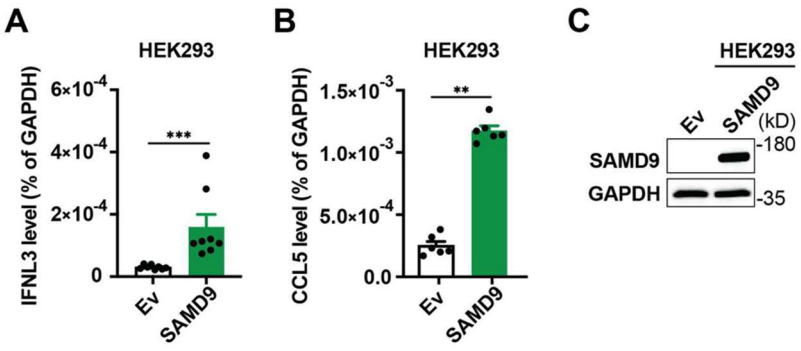

Supplementary Figure 3. SAMD9 induces IFN and CCL5 expression in HEK293 cells
(A-C) HEK293 cells transfected with Ev or SAMD9-Myc-DDK for 24 hr and the mRNA levels of IFNL3 (A) and CCL5 (B) measured by qRT-PCR, and the SAMD9 protein level measured by western blot (C). For all figures, experiments were repeated at least three times. Individual points in (A and B) represent independent experiments. Data are represented as mean ± SEM. Statistical significance in A-B calculated by unpaired two-tailed Student's *t* test: $^{**}P < 0.01$, $^{***}P < 0.001$.

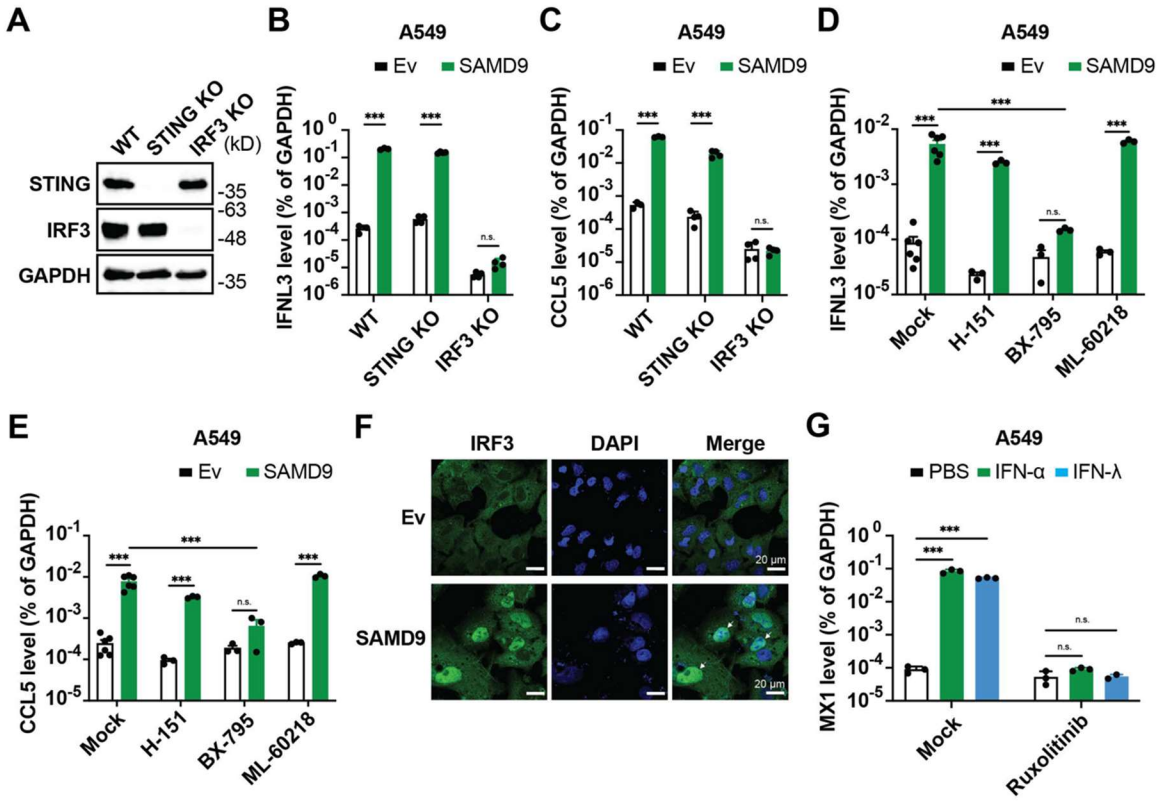

Supplementary Figure 4. SAMD9 induces IFN activation via the MAVS-TBK1-IRF3 pathway

(A) Validation of WT, pooled *STING* KO, and *IRF3* KO A549 cells by western blot with indicated antibodies.

(B-C) WT, *STING* KO, and *IRF3* KO A549 cells transfected with Ev or SAMD9-Myc-DDK for 24 hr and the mRNA levels of IFNL3 (B) and CCL5 (C) measured by qRT-PCR.

(D-E) A549 cells incubated with H-151, BX-795, or ML-60218 for 1 hr, then cells transfected with Ev or SAMD9-Myc-DDK for 24 hr and the mRNA levels of IFNL3 (D) and CCL5 (E) measured by qRT-PCR.

(F) A549 cells transfected with Ev or SAMD9-Myc-DDK for 24 hr, then fixed and stained for IRF3 (green) and nuclei (blue) by confocal microscopy.

(G) A549 cells incubated with ruxolitinib (10 μM) for 1hr, stimulated with IFN-α (100 U/ml) or IFN-λ (100 ng/ml) for 24 hr and the mRNA levels of MX1 measured by qRT-PCR. For all figures, experiments were repeated at least three times. Individual points in (B-E and G) represent independent experiments. Data are represented as mean ± SEM. Statistical significance calculated by two-way ANOVA with Sidak's multiple-comparisons tests (B-E and G): n.s., not significant, ***$P < 0.001$.

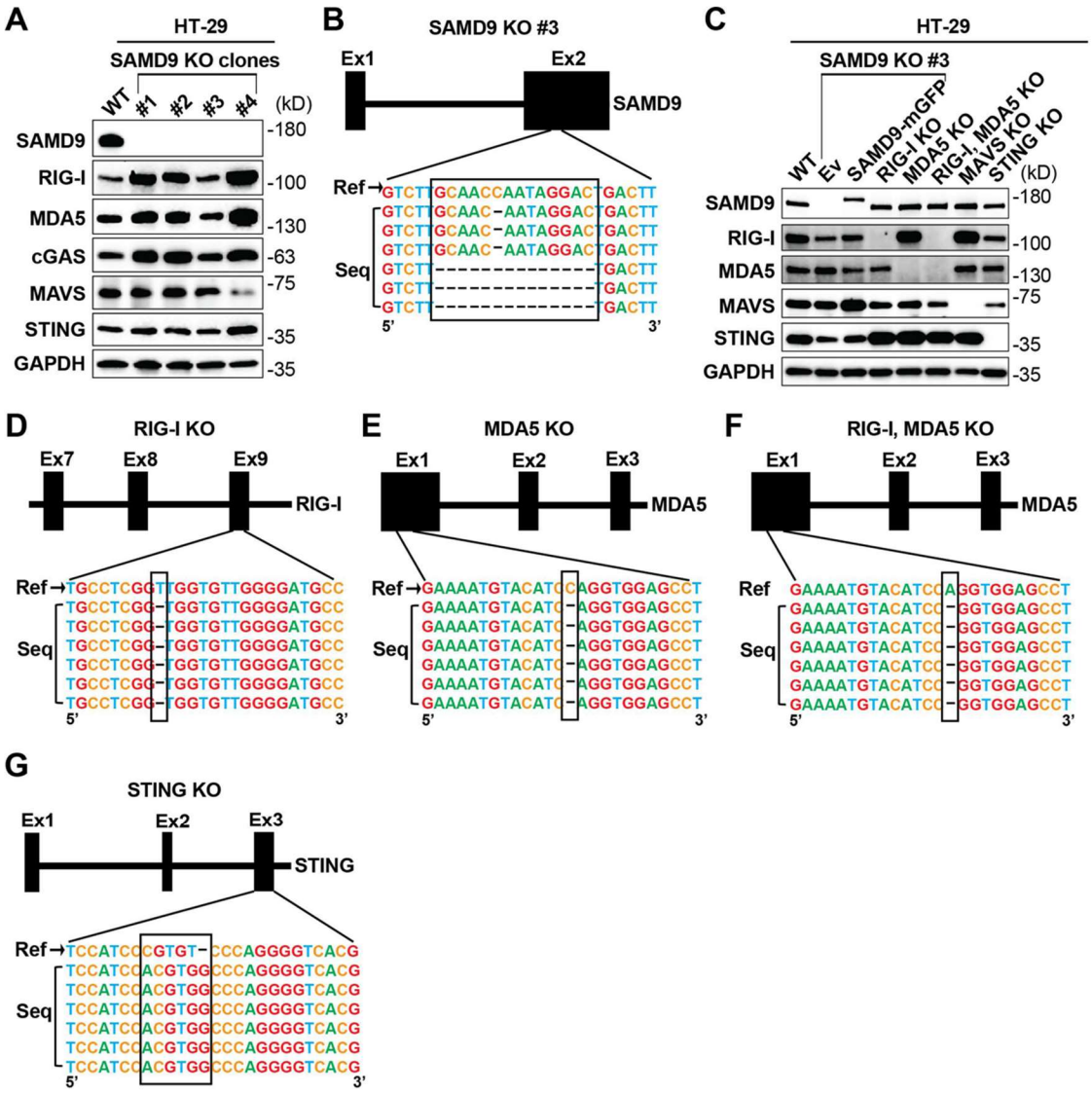

Supplementary Figure 5. Validation of SAMD9 and other innate immune gene knockout HT-29 cells

(A) Cell lysates of WT and different clones of *SAMD9* KO HT-29 cells resolved in SDS-PAGE gel and immunoblotted with indicated antibodies.

(B) Clone 3 of *SAMD9* KO HT-29 cells validated by Sanger sequencing.

(C) Validation of WT, Ev, SAMD9-mGFP add-back *SAMD9* KO, *RIG-I* KO, *MDA5* KO, *RIG-I MDA5* double KO, M*AVS* KO, *STING* KO HT-29 cells by western blot with indicated antibodies.

(D-G) *RIG-I* KO (D), *MDA5* KO (E), *RIG-I/MDA5* DKO generated from *RIG-I* KO cells (F), and *STING* KO (G) HT-29 cells validated by Sanger sequencing. For all figures, experiments were repeated at least three times.

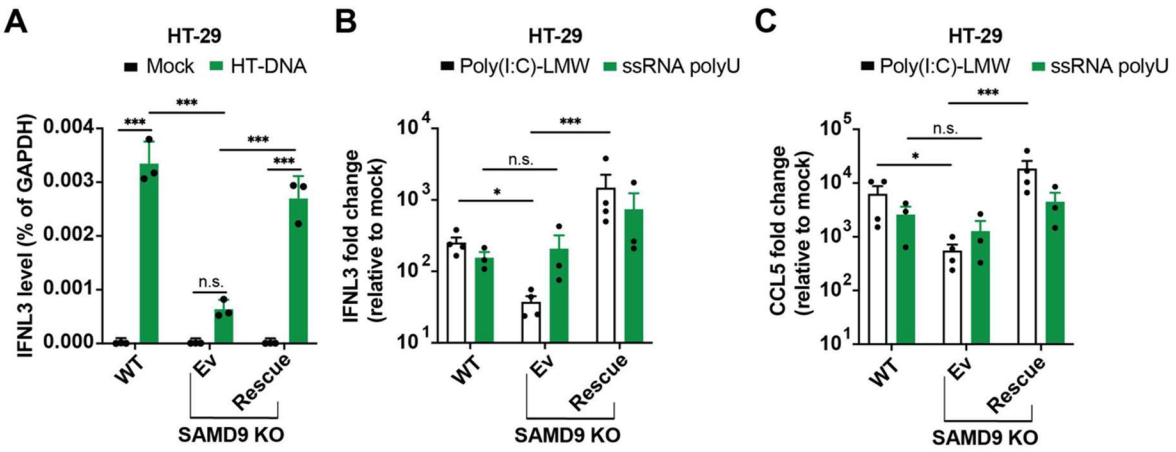

Supplementary Figure 6. IFN induction by cytosolic dsDNA and dsRNA is decreased in SAMD9 KO HT-29 cells

(A) WT and *SAMD9* KO complemented with Ev or SAMD9-mGFP (Rescue) HT-29 cells transected with herring testes DNA (HT-DNA) for 24 hr and the IFNL3 mRNA level examined by qRT-PCR.

(B-C) Similar to A except cells transfected with LMW poly(I:C) and single-stranded RNA polyuridine (ssRNA polyU) instead, the mRNA levels of IFNL3 (B) and CCL5 (C) measured by qRT-PCR. For all figures, experiments were repeated at least three times. Individual points in (A-B) represent independent experiments. Data are represented as mean ± SEM. Statistical significance in A-C calculated by two-way ANOVA with Sidak's multiple-comparisons tests: n.s., not significant, **P* < 0.05, ****P* < 0.001.

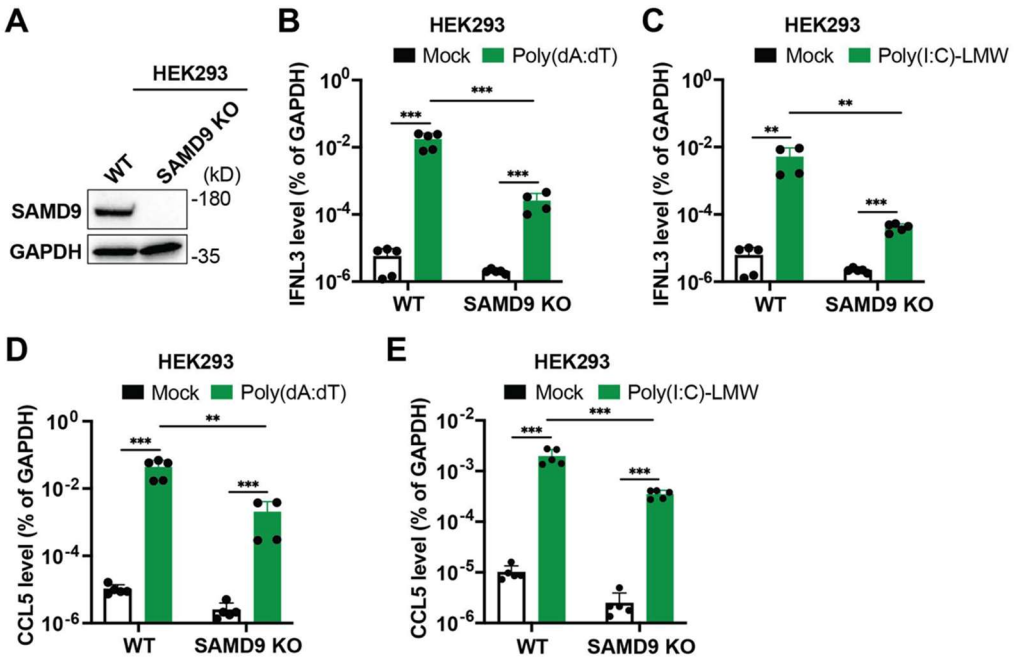

Supplementary Figure 7. IFNL3 and CCL5 expression is mediated by SAMD9 in response to cytosolic dsDNA and dsRNA stimulation in HEK293 cells

(A) *SAMD9* KO HEK293 cells validated by western blot.

(B-C) IFNL3 mRNA levels in poly(dA:dT) (B) or LMW poly(I:C) (C) (1 μg/ml) transfected *SAMD9* KO HEK293 cells measured by qRT-PCR.

(D-E) Similar to B-C except CCL5 mRNA level measured instead by qRT-PCR. For all figures, experiments were repeated at least three times. Individual points in (B-E) represent independent experiments. Data are represented as mean ± SEM. Statistical significance in B-E calculated by two-way ANOVA with Sidak's multiple-comparisons tests: $^{**}P < 0.01$, $^{***}P < 0.001$.

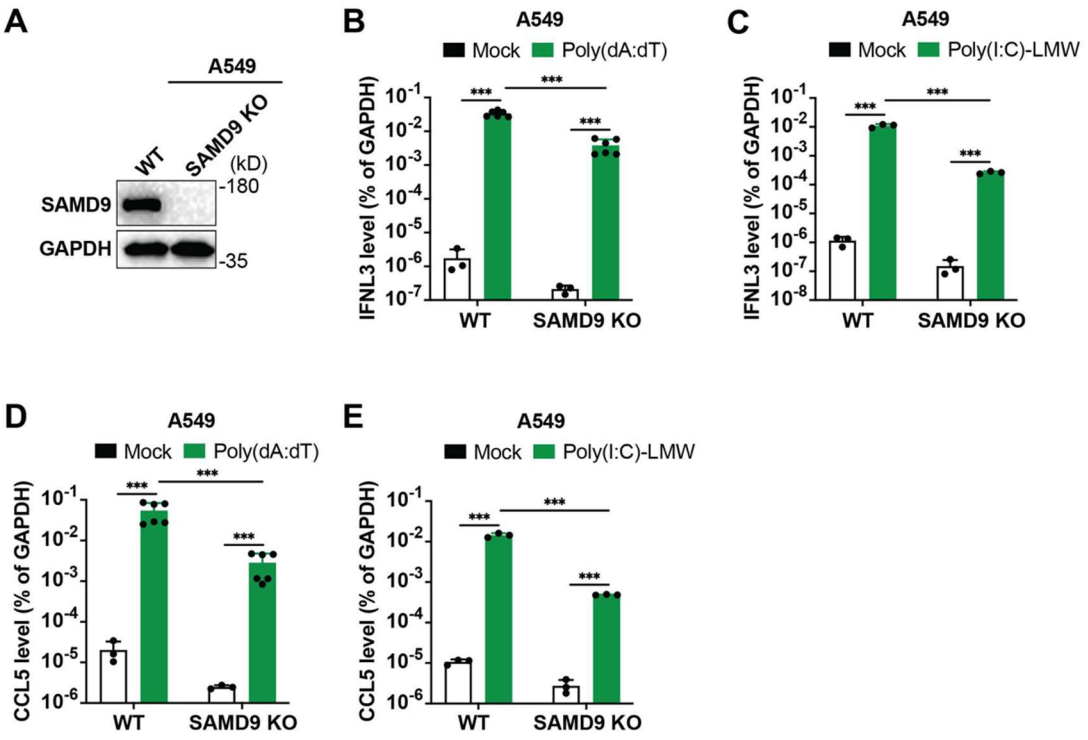

Supplementary Figure 8. IFNL3 and CCL5 expression is mediated by SAMD9 in response to cytosolic dsDNA and dsRNA stimulation in A549 cells

(A) *SAMD9* KO A549 cells validated by western blot.

(B-C) IFNL3 mRNA levels in poly(dA:dT) (B) or LMW poly(I:C) (C) (1 μg/ml) transfected *SAMD9* KO A549 cells measured by qRT-PCR.

(D-E) Similar to B-C except CCL5 mRNA level measured instead by qRT-PCR. For all figures, experiments were repeated at least three times. Individual points in (B-E) represent independent experiments. Data are represented as mean ± SEM. Statistical significance in B-E calculated by two-way ANOVA with Sidak's multiple-comparisons tests: ***$P < 0.001$.

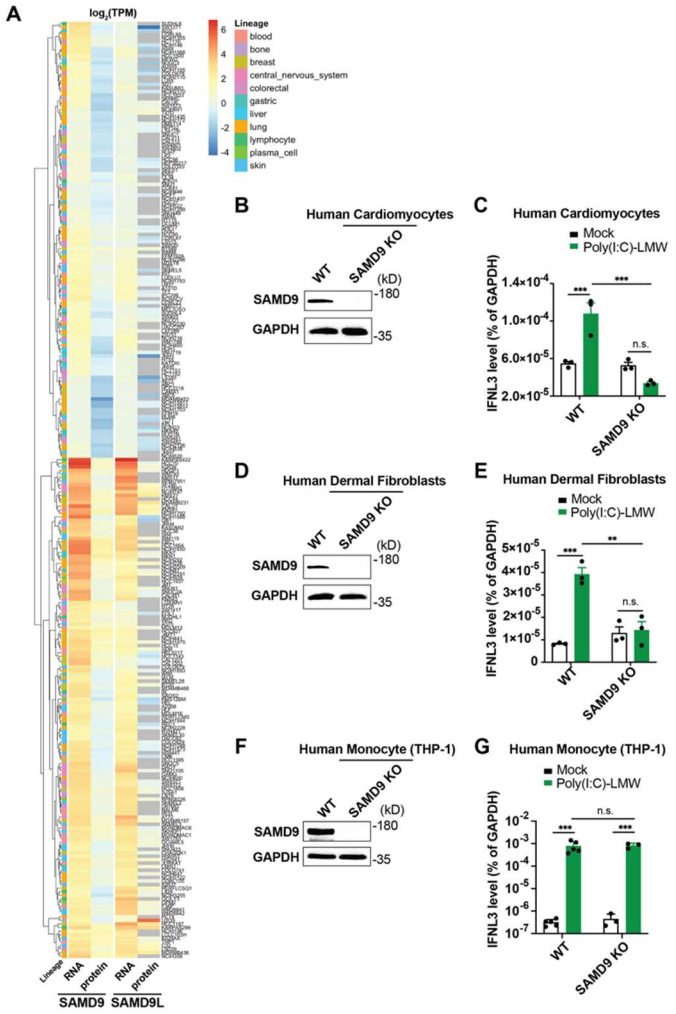

Supplementary Figure 9. SAMD9 mediates IFN responses in primary human cardiomyocytes and fibroblasts

(A) Heatmap of RNA and protein levels of SAMD9 and SAMD9L in human cell lines of different organ origins.

(B) Validation of *SAMD9* KO primary human cardiomyocytes by western blot.

(C) IFNL3 mRNA levels in LMW poly(I:C) (1 μg/ml) transfected WT or *SAMD9* KO primary human cardiomyocytes measured by qRT-PCR.

(D) Validation of *SAMD9* KO primary human dermal fibroblasts by western blot.

(E) IFNL3 mRNA levels in LMW poly(I:C) (1 μg/ml) transfected WT or *SAMD9* KO primary human dermal fibroblasts measured by qRT-PCR.

(F) Validation of pooled *SAMD9* KO human monocyte THP-1 cells by western blot.

(G) IFNL3 mRNA levels in LMW poly(I:C) (1 μg/ml) transfected WT or *SAMD9* KO human monocyte THP-1 cells measured by qRT-PCR. For all figures, experiments were repeated at least three times. Individual points in (C, E, and G) represent independent experiments. Data are represented as mean ± SEM. Statistical significance in C, E, and G calculated by two-way ANOVA with Sidak's multiple-comparisons tests: n.s., not significant, $^{**}P < 0.01$, $^{***}P < 0.001$.

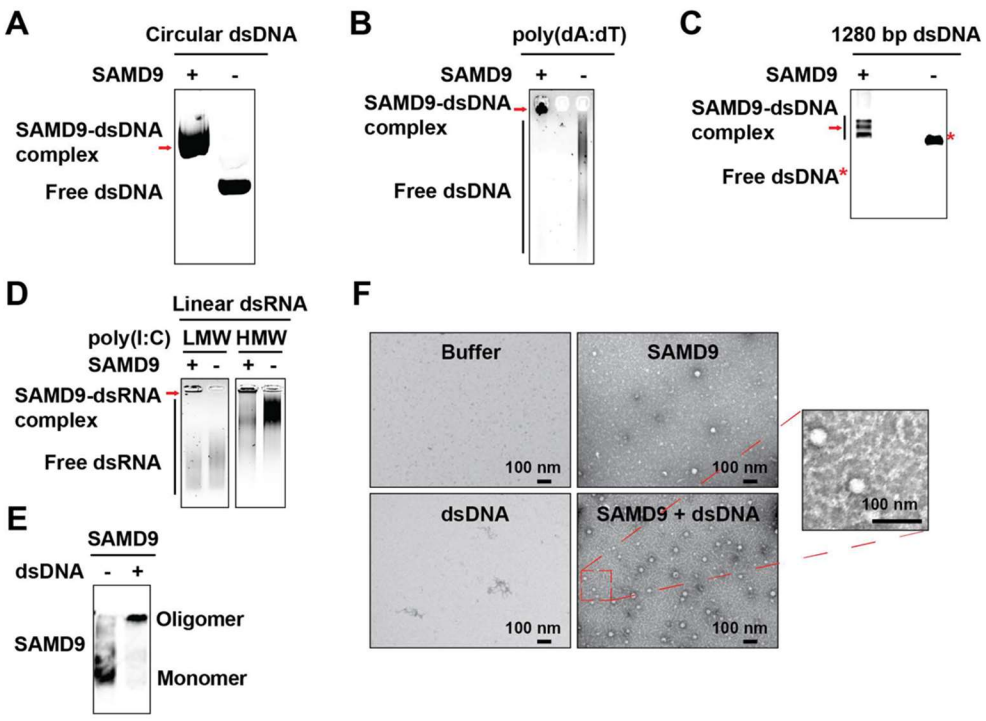

Supplementary Figure 10. SAMD9 binds to different forms of dsDNA and dsRNA
(A) EMSA of His-SAMD9 with circular dsDNA at a molar ratio of 8:1.
(B-C) EMSA of His-SAMD9 with poly(dA:dT) (B) or 1280-bp dsDNA (C).
(D) EMSA of His-SAMD9 with low molecular weight (LMW) or high molecular weight (HMW) poly(I:C).
(E) Native-PAGE electrophoresis of His-SAMD9 with or without circular dsDNA and detection by an anti-SAMD9 antibody.
(F) Representative electron micrographs of negatively stained SAMD9 in complex with circular dsDNA. For all figures, experiments were repeated at least three times.

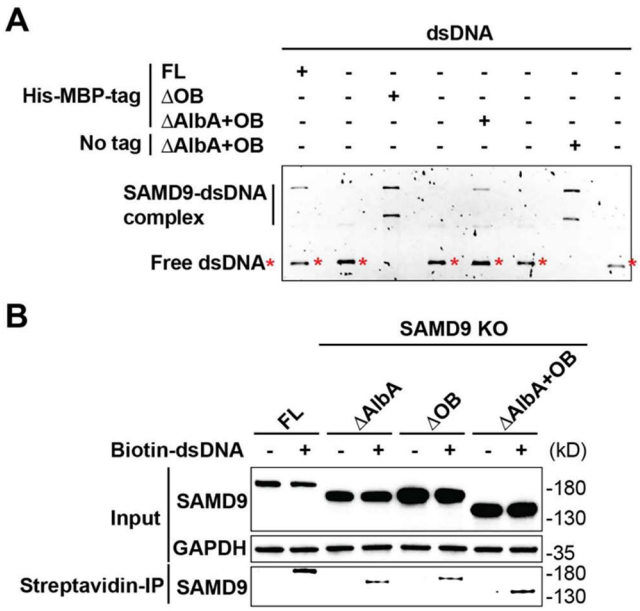

Supplementary Figure 11. SAMD9 binds to dsDNA independent of AlbA and OB-fold domains

(A) EMSA of His-MBP-tagged SAMD9 FL, ΔOB, ΔAlbA+OB, or non-tagged ΔAlbA+OB proteins with circular dsDNA.

(B) Immunoblotting analysis of streptavidin immunoprecipitates of cell lysates from WT HT-29 and *SAMD9* KO HT-29 cells complemented with FL, ΔAlbA, ΔOB, or ΔAlbA+OB incubated with biotinylated linear dsDNA. For all figures, experiments were repeated at least three times.

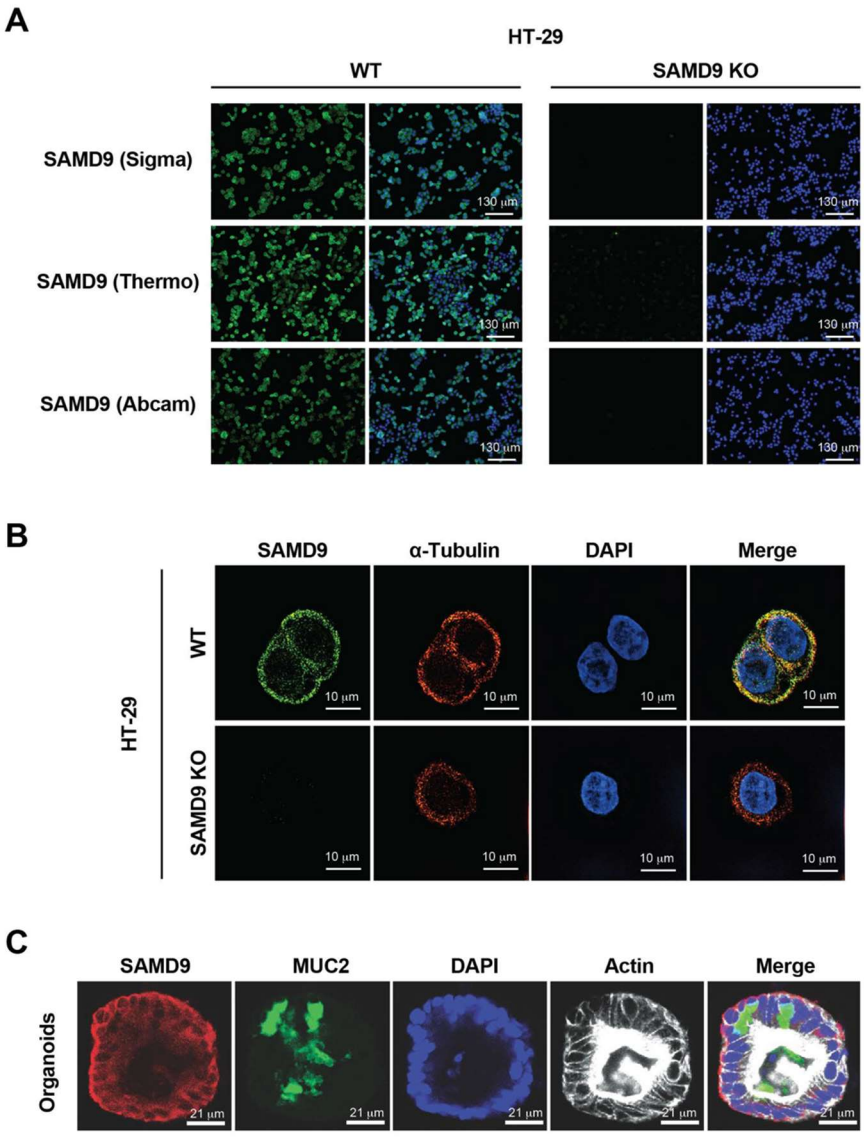

Supplementary Figure 12. SAMD9 is present in the cytosol
(A) WT and *SAMD9* KO HT-29 cells fixed and stained for endogenous SAMD9 (green) with antibodies from different vendors and nuclei (blue) by fluorescence microscopy.
(B) WT and *SAMD9* KO HT-29 cells fixed and stained for SAMD9 (green), α-tubulin (red), and nuclei (blue) by super-resolution microscopy.
(C) Human ileal organoids fixed and stained for SAMD9 (red), MUC2 (green), nuclei (blue), and actin (grey) by confocal microscopy. For all figures, experiments were repeated at least three times.

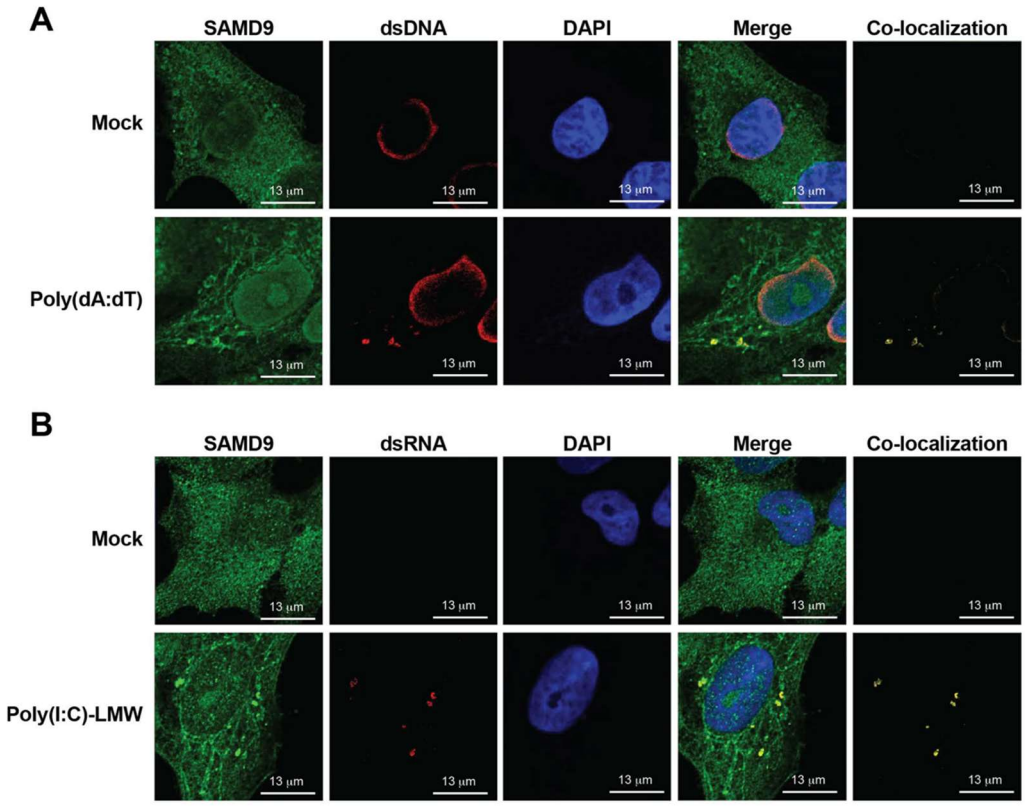

Supplementary Figure 13. SAMD9 colocalizes with cytosolic dsDNA and dsRNA
(A) A549 cells transfected with poly(dA:dT) (10 μg/ml) for 8 hr, then fixed and stained for SAMD9 (green), dsDNA (red), nuclei (blue), and colocalization (yellow) by confocal microscopy.
(B) Similar to A except LMW poly(I:C) was transfected instead of poly(dA:dT). For all figures, experiments were repeated at least three times.

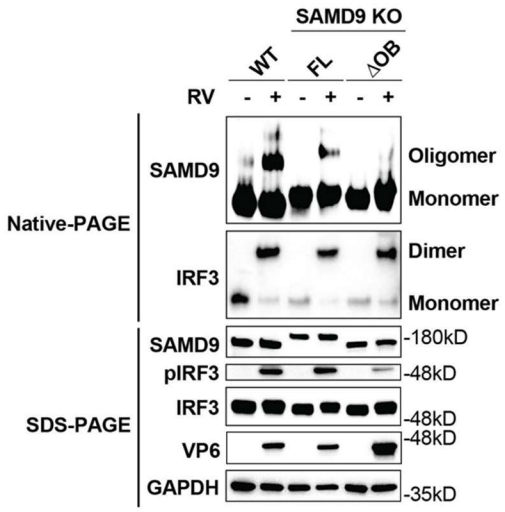

Supplementary Figure 14. The OB-fold domain is important for SAMD9 oligomerization upon RV infection

WT HT-29 cells, and *SAMD9* KO HT-29 cells complemented with SAMD9-mGFP (FL) or SAMD9-ΔOB-mGFP (ΔOB) infected with RV (MOI=3) for 8 hr, and cell lysates harvested for native-PAGE or SDS-PAGE electrophoresis with indicated antibodies. This experiment was repeated at least three times.

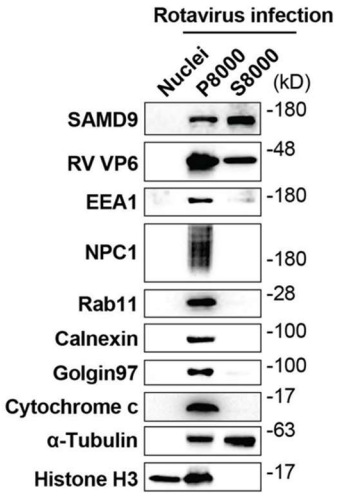

Supplementary Figure 15. SAMD9 is partially redistributed upon RV infection
A549 cells infected with rotavirus (MOI=3) for 8 hr, then the nuclear, pellet (P8000), and supernatant (S8000) fractions from centrifugation of 8,000*g* of homogenized A549 cells immunoblotted with indicated antibodies. This experiment was repeated at least three times.

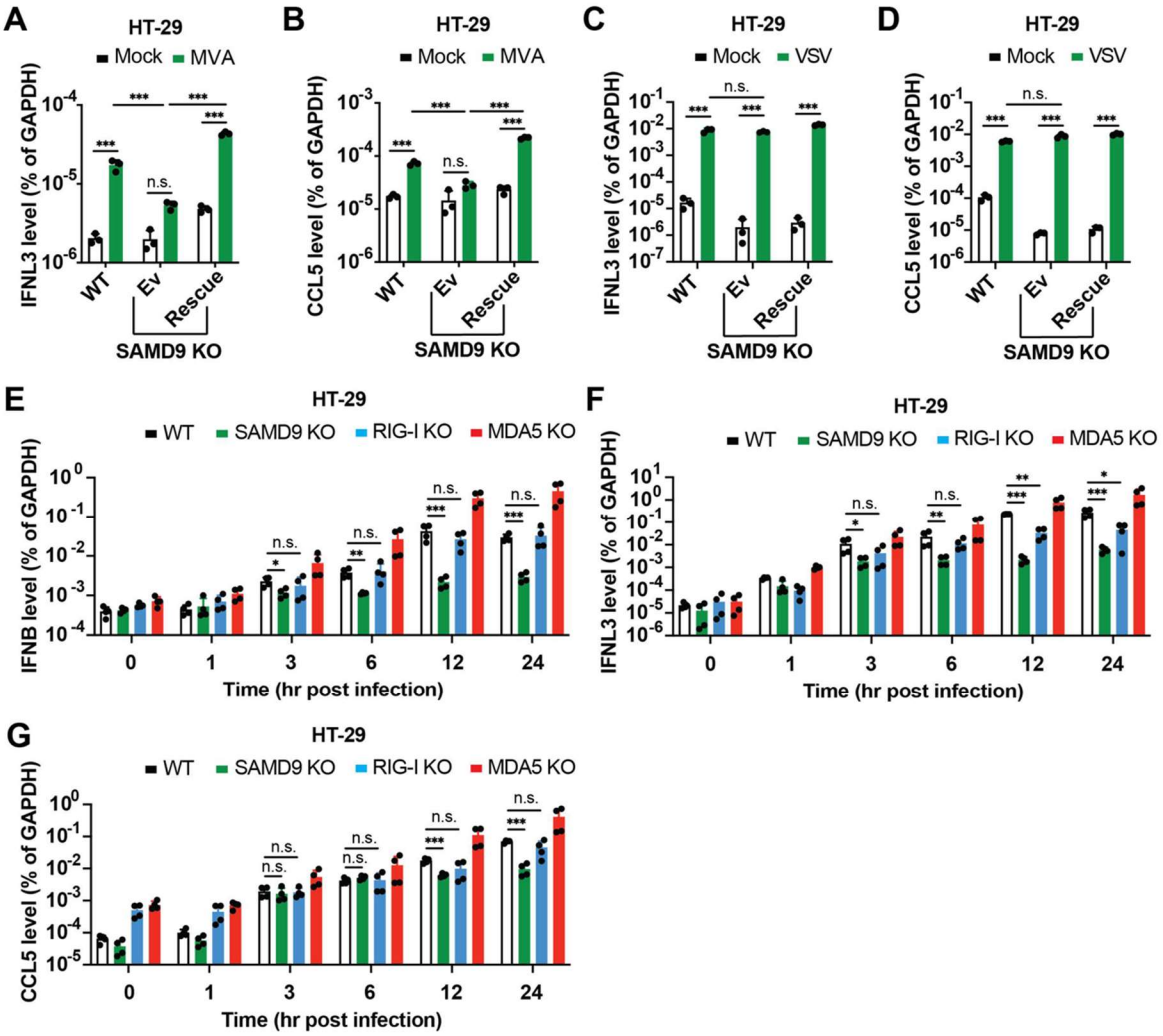

Supplementary Figure 16. CCL5 induction by dsRNA or dsDNA virus infections is reduced in SAMD9 KO cells

(A-B) WT and *SAMD9* KO complemented with Ev or SAMD9-mGFP (Rescue) HT-29 cells infected with modified vaccinia virus (MVA) (MOI=0.01) for 24 hr, the IFNL3 (A) and CCL5 (B) mRNA levels measured by qRT-PCR.

(C-D) Cells were infected with vesicular stomatitis virus (VSV) (MOI=0.01) for 24 hr and the IFNL3 (C) and CCL5 (D) mRNA levels measured by qRT-PCR.

(E-G) WT, *SAMD9* KO, *RIG-I* KO, and *MDA5* KO HT-29 cells infected with RV for indicated time points, the mRNA levels of IFNB (H), IFNL3 (I) and CCL5 (J) measured by qRT-PCR. For all figures, experiments were repeated at least three times. Individual points in A-G represent independent experiments. Data are represented as mean ± SEM. Statistical significance in A-G calculated by two-way ANOVA with Sidak's multiple-comparisons tests: n.s., not significant, **P* < 0.05, ***P* < 0.01, ****P* < 0.001.

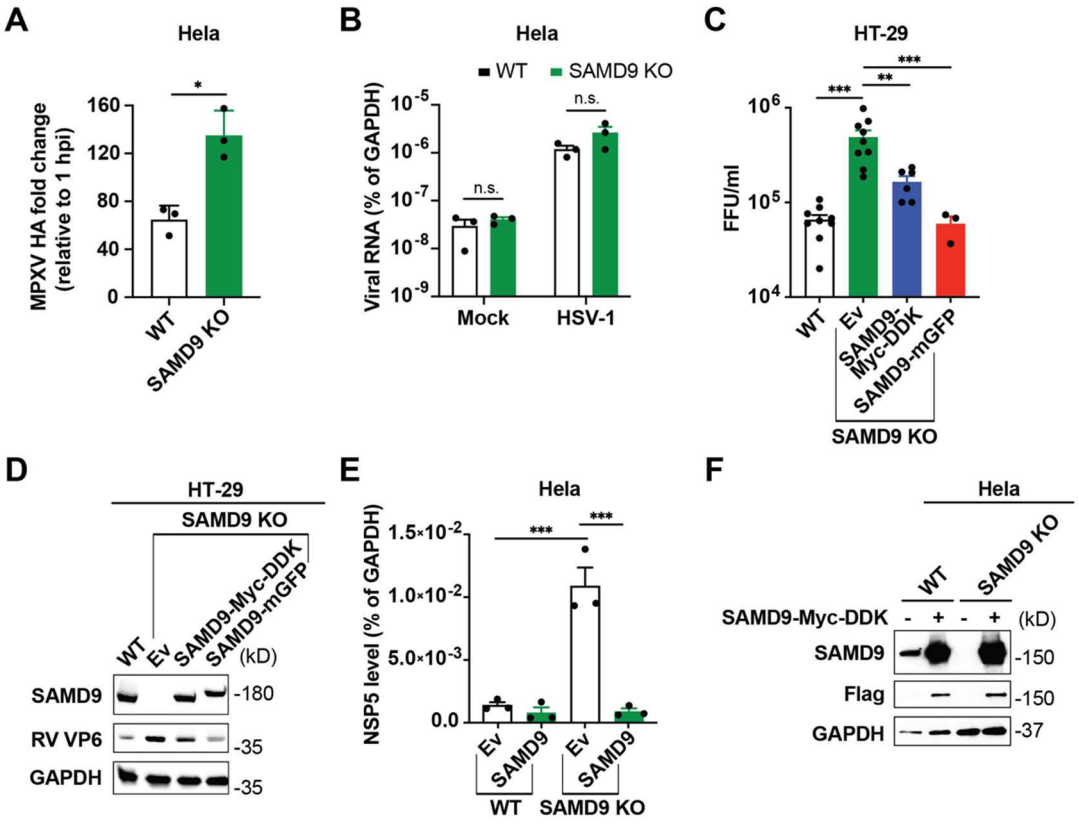

Supplementary Figure 17. Monkeypox virus and RV infections are enhanced in SAMD9 KO cells

(A) WT and *SAMD9* KO Hela cells infected with monkeypox virus (MOI=0.1) for 24 hr and the mRNA level of monkeypox virus HA measured by qRT-PCR.

(B) WT and *SAMD9* KO Hela cells infected with herpes simplex virus type 1 (HSV-1) (MOI=0.1) for 24 hr and the mRNA level of HSV-1 virus measured by qRT-PCR.

(C) WT and *SAMD9* KO complemented with Ev, SAMD9-Myc-DDK (pooled), or SAMD9-mGFP (single clone) HT-29 cells infected with rotavirus (MOI=0.1) for 24 hr and the infectious progeny viruses measured by focus forming unit (FFU) assays.

(D) Western blot analysis of cell lines in (C) with indicated antibodies.

(E-F) WT and *SAMD9* KO Hela cells transfected with Ev or SAMD9-Myc-DDK for 48 hr, infected with rotavirus (MOI=0.1) for 24 hr, and the mRNA level of viral transcript NSP5 measured by qRT-PCR (E), and the transfection efficiency of SAMD9-Myc-DDK examined by western blot with indicated antibodies (F). For all figures, experiments were repeated at least three times. Individual points in (A-C and E) represent independent experiments. Data are represented as mean ± SEM. Statistical significance calculated by unpaired two-tailed Student's *t* test (A), two-way ANOVA with Sidak's multiple-comparisons tests (B), and one-way ANOVA with Dunnett's post-test (C and E): n.s., not significant, **P* < 0.05, ***P* < 0.01, ****P* < 0.001.

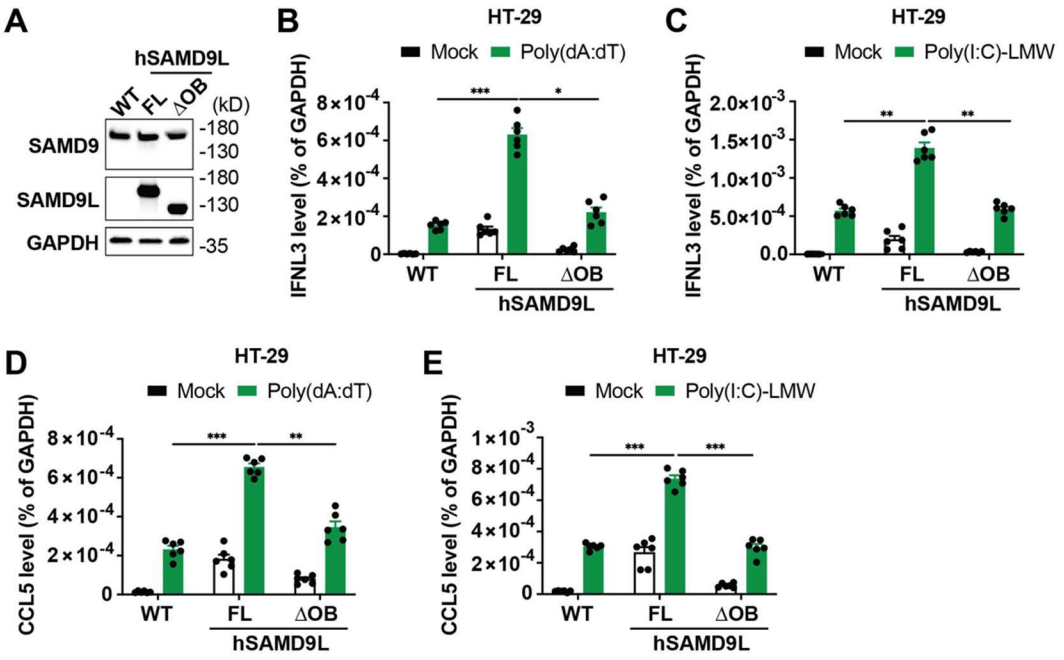

Supplementary Figure 18. SAMD9L OB-fold domain is important for IFNL3 and CCL5 induction

(A) Western blot analysis of WT HT-29, or WT cells complemented with hSAMD9L and hSAMD9L-ΔOB with indicated antibodies.

(B-C) HT-29 cells or those stably expressing full-length (FL) or ΔOB human SAMD9L transfected with poly(dA:dT) (B) or LMW poly(I:C) (C) (1 μg/ml) for 24 hr and the IFNL3 mRNA level measured by qRT-PCR.

(D-E) WT HT-29 cells or WT cells complemented with hSAMD9L, hSAMD9L-ΔOB transfected with poly(dA:dT) (D) or LMW poly(I:C) (E) (1 μg/ml) for 24 hr, and the CCL5 mRNA level measured by qRT-PCR. For all figures, experiments were repeated at least three times. Individual points in B-E represent independent experiments. Data are represented as mean ± SEM. Statistical significance in B-E calculated by two-way ANOVA with Sidak's multiple-comparisons tests: **P* < 0.05, ***P* < 0.01, ****P* < 0.001.

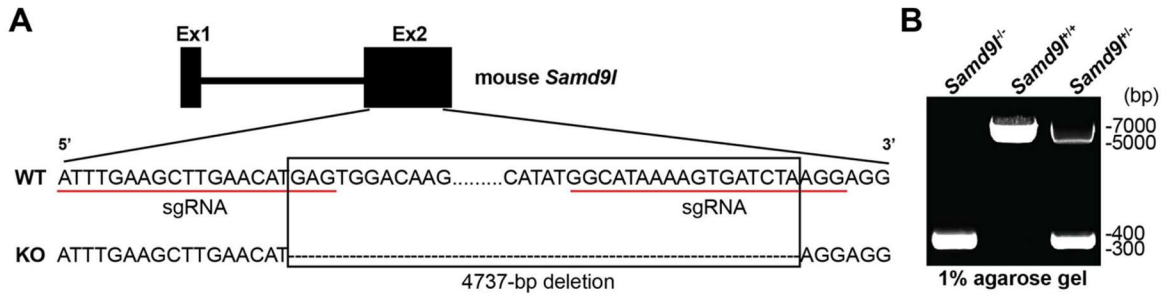

Supplementary Figure 19. Generation and genotyping of *Samd9l*$^{-/-}$ mice
(A) Schematic representation of the CRISPR-Cas9 targeting strategy used for generating *Samd9l*$^{-/-}$ mice. Single guide RNA (sgRNA) binding sequences highlighted by underlines. (B) A representative genotyping PCR result using genomic DNA extracted from tails of *Samd9l*$^{+/+}$, *Samd9l*$^{+/-}$, and *Samd9l*$^{-/-}$ mice. For all figures, experiments were repeated at least three times.

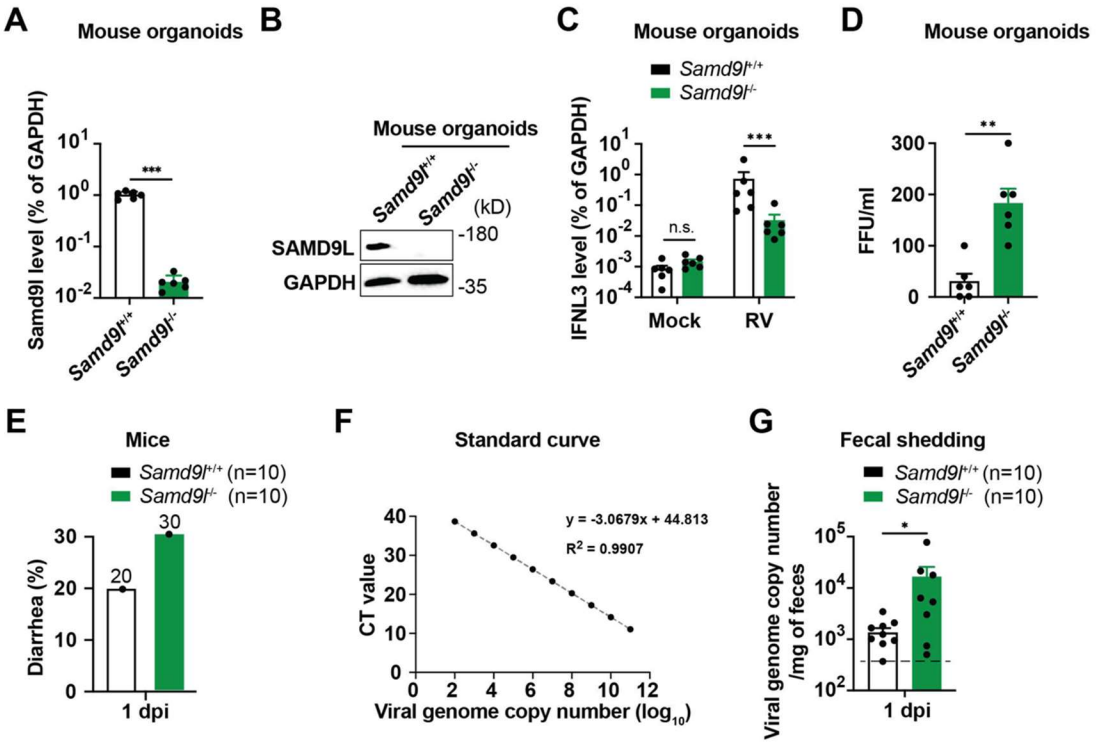

Supplementary Figure 20. *Samd9l*$^{-/-}$ mice support increased RV replication and pathogenesis

(A) Samd9l mRNA level of *Samd9l*$^{+/+}$ and *Samd9l*$^{-/-}$ ileal organoids measured by qRT-PCR.

(B) Western blot analysis of *Samd9l*$^{+/+}$ and *Samd9l*$^{-/-}$ ileal organoids with indicated antibodies.

(C-D) *Samd9l*$^{+/+}$ or *Samd9l*$^{-/-}$ murine ileal organoids infected by RV (MOI=0.1) for 24hr and the IFNL3 mRNA level measured by qRT-PCR (C) or infectious virus titers measured by focus forming unit (FFU) assays (D).

(E) Five-day-old *Samd9l*$^{+/+}$ and *Samd9l*$^{-/-}$ cohoused neonatal littermates orally inoculated with murine RV (1.5 x 10^3 FFUs per mouse) and the percentage of diarrhea development recorded at 1 dpi.

(F) A standard curve of qRT-PCR assays that measure RV NSP5 copy numbers. Serially diluted RV genome copies in $\log_{10}$ values in the X-axis and the threshold cycle (CT) values in the Y-axis.

(G) Five-day-old *Samd9l*$^{-/-}$ neonatal mice and *Samd9l*$^{+/+}$ littermate controls orally infected with murine RV (1.5 x 10^3 FFU per mouse) and RV genome copy numbers in the feces collected at 1 dpi quantified by an absolute qRT-PCR assay. For all figures, experiments were repeated at least three times. Individual points in (A, C and D) represent independent experiments, and in G represent individual mouse. Data are represented as mean ± SEM. Statistical significance calculated by unpaired two-tailed Student's *t* test (A, D, and G), two-way ANOVA with Sidak's multiple-comparisons tests (C), and nonlinear regression fit curve (F): n.s., not significant., *P < 0.05, **P < 0.01, ***P < 0.001.

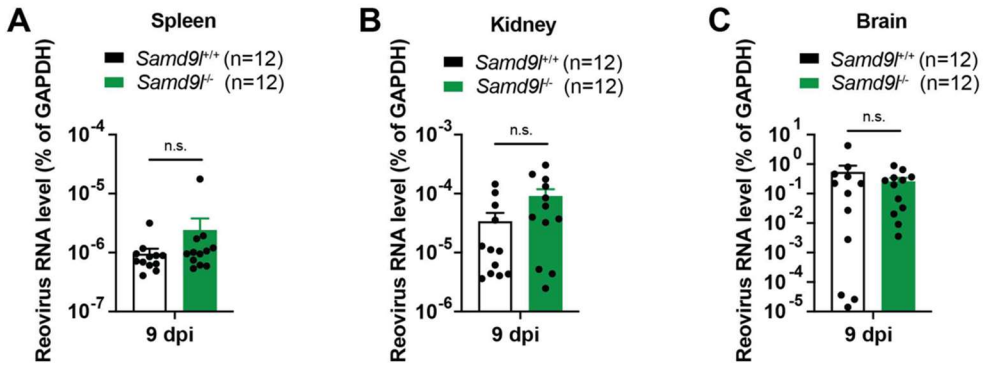

Supplementary Figure 21. Reovirus loads in *Samd9l*$^{-/-}$ neonatal mice tissues
(A-C) Three-day-old *Samd9l*$^{+/+}$ and *Samd9l*$^{-/-}$ neonatal mice intraperitoneally injected with reovirus (1 x 10^4 PFU per mouse). RNA extracted from spleen (A), kidney (B) and brain (C) collected at 9 dpi, and reovirus mRNA levels measured by qRT-PCR. For all figures, experiments were repeated at least three times. Individual points in A-C represent individual mouse. Data are represented as mean ± SEM. Statistical significance calculated by unpaired two-tailed Student's *t* test (A-C): n.s., not significant.

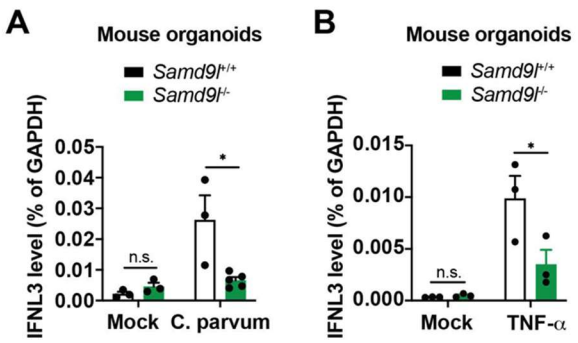

Supplementary Figure 22. IFNL3 induction by *Cryptosporidium parvum* and TNF-α stimulation is reduced in *Samd9l*$^{-/-}$ intestinal organoids

(A) *Samd9l*$^{+/+}$ and *Samd9l*$^{-/-}$ ileal organoids infected by *Cryptosporidium parvum* (*C. parvum*; 2 x 10^5 oocytes) for 24 hr and IFNL3 mRNA level measured by qRT-PCR.

(B) Organoids stimulated with mouse TNF-α (100 ng/ml) for 24 hr and IFNL3 mRNA level measured by qRT-PCR. For all figures, experiments were repeated at least three times. Individual points in A and B represent independent experiments. Data are represented as mean ± SEM. Statistical significance in A and B calculated by two-way ANOVA with Sidak's multiple-comparisons tests: n.s., not significant., *P < 0.05.

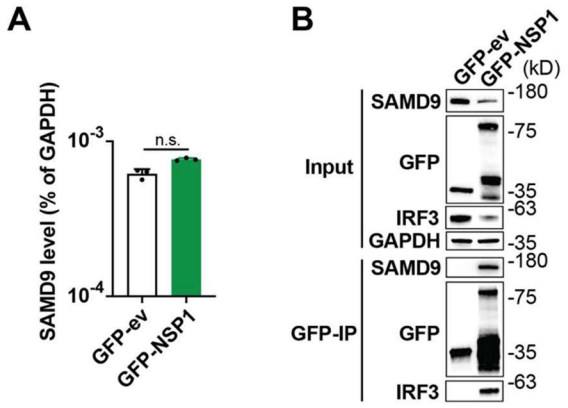

Supplementary Figure 23. SAMD9 interacts with RV NSP1

(A) HEK293 cells transfected with GFP-ev or GFP-NSP1 for 48 hr and SAMD9 mRNA level measured by qRT-PCR.

(B) Immunoblotting analysis of anti-GFP antibody immunoprecipitates of cell lysates from HEK293 cells transfected with GFP-ev or GFP-NSP1. For all figures, experiments were repeated at least three times. Individual points in A represent independent experiments. Data are represented as mean ± SEM. Statistical significance in A calculated by unpaired two-tailed Student's t test: n.s., not significant.

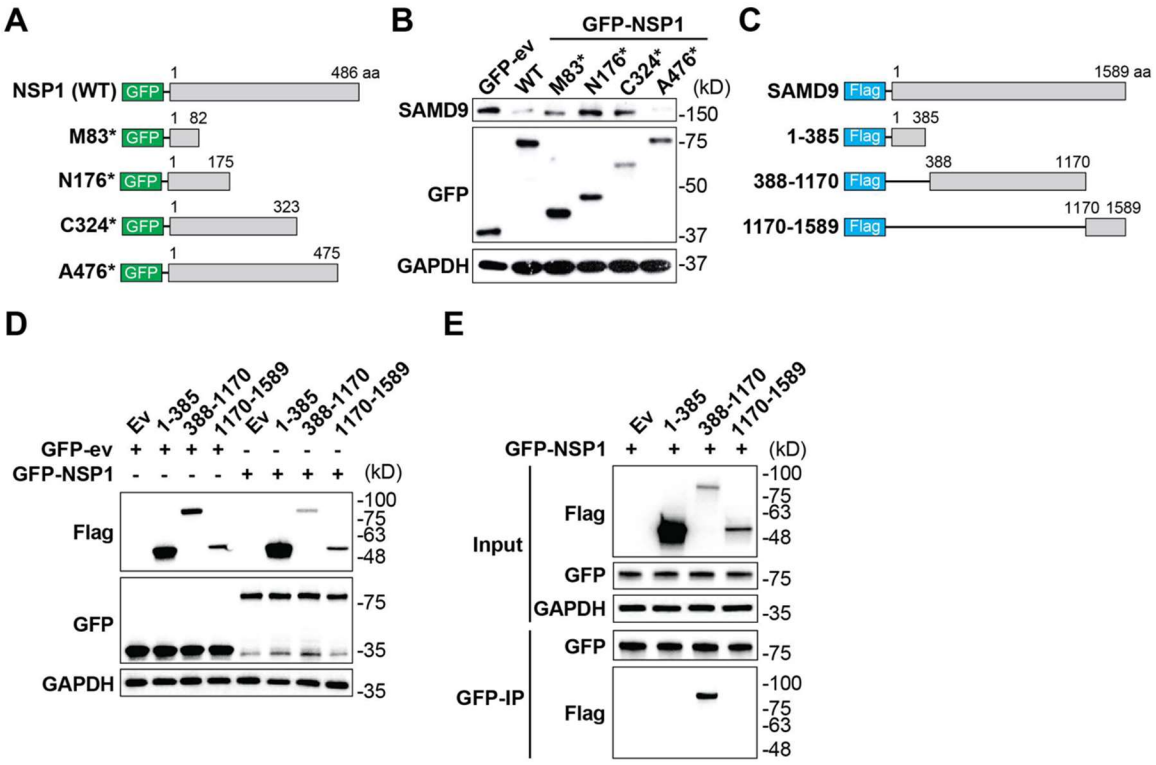

Supplementary Figure 24. SAMD9 388-1170 aa domain is targeted by RV NSP1

(A) Schematic representation of WT or mutant NSP1 constructs.

(B) HEK293 cells transfected with GFP-ev, GFP-tagged NSP1 (WT), or NSP1 mutants for 48 hr and cell lysates harvested for SDS-PAGE electrophoresis with indicated antibodies.

(C) Schematic representation of N-terminally 3× Flag-tagged SAMD9 or mutants.

(D) HEK293 cells co-transfected with GFP-ev or GFP-NSP1 and Flag-tagged ev or SAMD9 mutants for 48 hr and cell lysates harvested for SDS-PAGE electrophoresis with indicated antibodies.

(E) Immunoblotting analysis of anti-GFP antibody immunoprecipitates of cell lysates from HEK293 cells co-transfected with Flag-tagged ev or SAMD9 mutants and GFP-NSP1. For all figures, experiments were repeated at least three times.

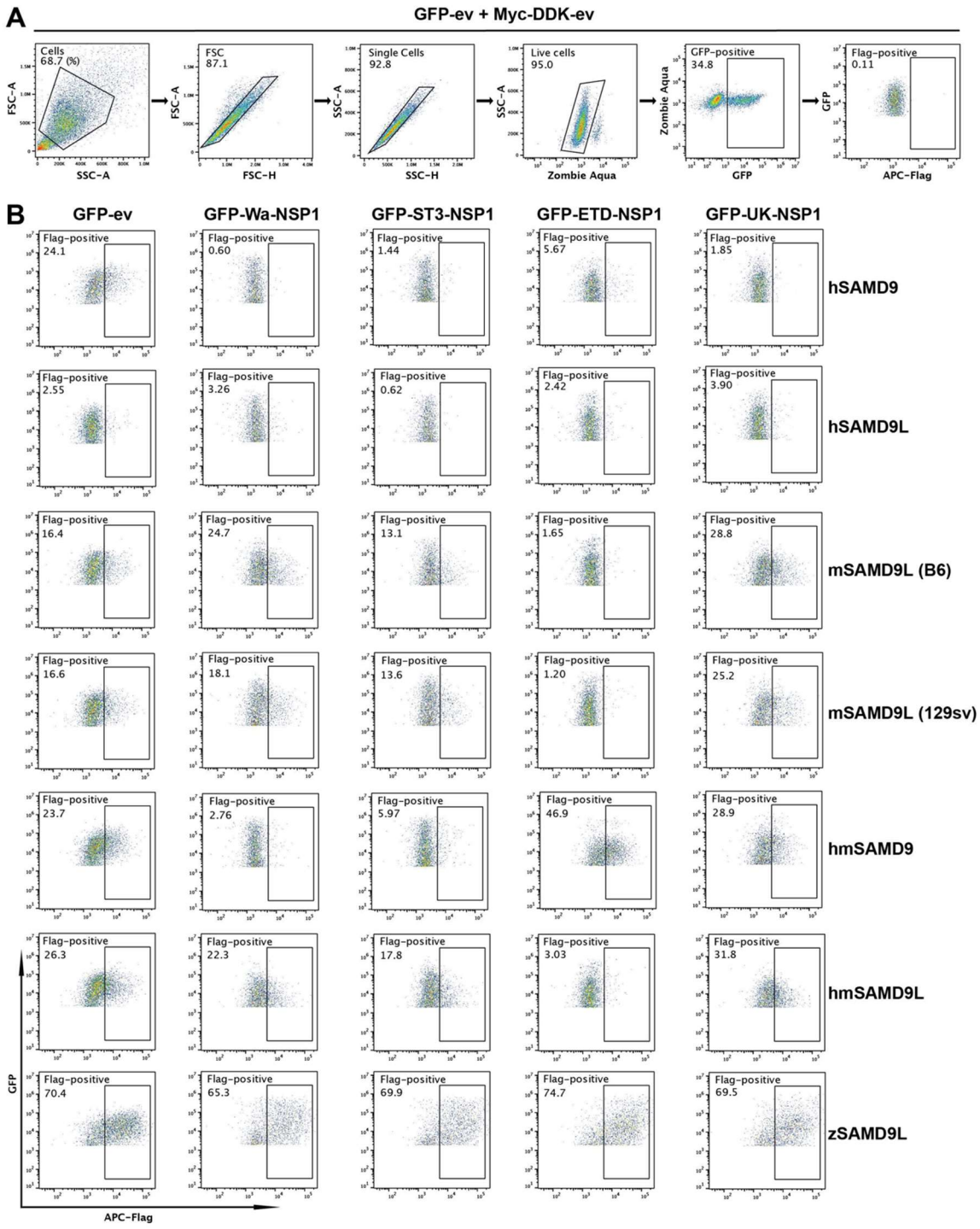

Supplementary Figure 25. SAMD9 protein level analysis by flow cytometry
(A) Gating strategy of flow cytometry to quantify the percentage of Flag-tagged SAMD9 positive cells within GFP-positive populations.
(B) Representative flow cytometry images of the percentage of Flag-tagged positive cells expressing SAMD9 or SAMD9L from different species in GFP-positive NSP1-expressing populations. For all figures, experiments were repeated at least three times.

Supplementary Table 1. QPCR and CRISPR Primer information

GAPDH	Forward	GGAGCGAGATCCCTCCAAAAT
	Reverse	GGCTGTTGTCATACTTCTCATGG
IFB	Forward	ATGACCAACAAGTGTCTCCTCC
	Reverse	GGAATCCAAGCAAGTTGTAGCTC
IFNL3	Forward	TAAGAGGGCCAAAGATGCCTT
	Reverse	CTGGTCCAAGACATCCCCC
CCL5	Forward	CCAGCAGTCGTCTTTGTCAC
	Reverse	CTCTGGGTTGGCACACACTT
CXCL1O	Forward	GTGGCATTCAAGGAGTACCTC
	Reverse	TGATGGCCTTCGATTCTGGATT
MX1	Forward	GTGGCTGAGAACAACCTGTG
	Reverse	GGCATCTGGTCACGATCCC
NSP5	Forward	CTGCTTCAAA CGATCCACTCAC
	Reverse	TGAATCCATAGACACGCC
	Probe	CY5/TCAAATGCAGTTAAGACAAATGCAGACGCT /IABRQSP
Reovirus T1F	Forward	GCATCCATTGTAAATGACGAGTCTG
	Reverse	CTTGAGATTAG CTCTAGCATCTTC TG
IAV-A1	Forward	AAGACCAATCCTGTCACCTCTGA
	Reverse	CAAAGCGTCTACGCTGCAGTCC
VSV-N	Forward	GATAGTACCGGAGGATTGACGACTA
	Reverse	TCAAACCATCCGAGCCATTC
CHIKV	Forward	AAGCTCCGCGTCCTTTACCAAG
	Reverse	CCAAATTGTCCTGGTCTTCCT
ZIKV	Forward	TTGGTCATGATACTGCTGATTGC
	Reverse	CCTTCCACAAAGTCCCTATTGC
HAstV	Forward	CAGGCTTTACCCACAT
	Reverse	TACAGACATGTGCATGAATGG
AdV	Forward	GACATGACTTTCGAGGTCGATCCCATGG
	Reverse	CCGGCTGAGAAGGGTGTGCGCAGGTA
MVA	Forward	GGCAA TGGATTCAGGGATATAC
	Reverse	ATTTATGAATAATCCGCCAGTTAC
HSV-1 ICP27	Forward	TTTCTCCAGTGCTACCTGAAGG
	Reverse	TCAACTCGCAGACACGACTCG
Mouse Gapdh	Forward	TCTGGAAAGCTGTGCCGTG
	Reverse	CCAGTGAGCTTCCCGTTCAG
Mouse Ifnl3	Forward	AGCTGCAGGCCTTCAA AAAG
	Reverse	TGGGAGTGAATGTGGCTCAG
SAMD9	20nt-sgRNA	CGAGAAGTCTTGCAACCAAT
	Sequencing Forward	GCAGGAGAAACCTAGTAGC
	Sequencing Reverse	GTGAACAAGTCTTTCCAGTC

STING	20nt- sgRNA	GTGACCCCTGGGACACGGGA
	Sequencing Forward	GAAAGGGGAACTGGGAG
	Sequencing Reverse	AGTCACCT GGAGTGGATGT
RIG-I	20nt- sgRNA	GGCATCCCCAACACCAACCG
	Sequencing Forward	GCATTATGTGCCTCCATG
	Sequencing Reverse	GGGATGAGAGCTCAGTTAGAG
MDA5	20nt- sgRNA	GGTGAAAATGTACATCCAGG
	Sequencing Forward	CTGCTTCTCTAAGTGGGCAG
	Sequencing Reverse	TGAGCTCAGGGTTCATGTAG